Chemistry–A European Journal
Research Article
doi.org/10.1002/chem.202200332
Chemistry Europe
European Chemical Societies Publishing
www.chemeurj.org

2-Aminoalkylgold Complexes: The Putative Intermediate in Au-Catalyzed Hydroamination of Alkenes Does Not Protodemetalate

Joël Gubler[+],[a] Mitar Radić[+],[a] Yannick Stöferle,[a] and Peter Chen*[a]

Abstract: Au-catalyzed hydroamination proceeds well for alkynes but not alkenes. We report gas-phase binding energies of alkenes and alkynes to a cationic Au center, which indicate that differences in binding are not the origin of the disparate chemical behavior. We further report the synthesis and characterization of 2-aminoalkylgold complexes, which would be the intermediates in a hypothetical Au-catalyzed hydroamination of styrene. The reactivity of the well-characterized and isolable complexes reveals that protonation or alkylation of the 2-aminoalkylgold complexes results in amine elimination in solution, and in the gas phase, indicating that the failure of Au-catalyzed alkene hydroamination derives from a non-competitive protodeauration step. We analyze possible transition states for the protodeauration, and identify an insufficiently strong Au-proton interaction as the reason that the transition states lie too high in energy to compete.

Introduction

Occupying a vast part of chemical space, amines have been continuously situated at the focus of synthetic interest. Hydroamination, a formal addition of an amine to an unsaturated carbon-carbon bond, represents a conceptually obvious methodology aiming for their preparation: its starting materials are bulk chemicals and analogous hydrofunctionalizations are widely employed reactions. Among other transition metals, gold catalysis emerged as a particularly potent platform for the development of catalysts carrying a potential to enable catalytic hydroaminations.[1,2] This can be related to the notion that the advent of the gold catalysis seen in the past two decades featured one more general and particularly prominent application of gold: the activation of unsaturated carbon-carbon bonds for the addition of N- and O-nucleophiles.

While much earlier mechanistic work has sought to differentiate between two possible pathways by which the C–N bond is formed, the inner-sphere mechanism with coordination of the amine nucleophile to the gold center on which the substrate is already bound, and the outer-sphere mechanism in which the substrate bound on gold is activated for direct attack by the amine nucleophile, the consensus has been reached that the C–N bond formation most likely proceeds by the outer-sphere mechanism, depicted for the general case in Scheme 1.[3,4] In the present work, we seek to address the subsequent steps in the catalytic cycle with special attention given to the question of chemoselectivity among potential substrates.

While Scheme 1 shows a hypothetical catalytic cycle for the hydroamination of alkenes, analogous elementary steps apply to hydroamination of alkynes. However, the reactivity of alkenes and alkynes in gold-catalyzed reactions is generally different, alkynes reacting preferentially, even in the presence of alkenes. In the classical example by Echavarren, 1,6-enynes underwent skeletal rearrangements resulting in products whose generation can be rationalized only by invoking chemoselectivity for alkyne functionality.[5] Furthermore, hydroamination of alkenes itself is, in general, less successful than that of alkynes.[6] This bias had been originally attributed to different binding constants of gold-alkyne and gold-alkene complexes. Following computational and experimental evidence, this essentially thermodynamic explanation has been questioned in several reports, re-opening the issue of the actual origin of the chemoselectivity for alkynes. This lead to the notion that the observed alkynophilicity could in fact arise from the kinetic differences.[7]

We report herein an experimental and computational study in which we *i*) revisit and re-measure binding energies of gold-alkyne and gold-alkene complexes by conducting energy-resolved collision-induced dissociation experiments using our customized mass spectrometer; *ii*) prepare and characterize hitherto unreported 2-aminoalkyl gold(I)-complexes and *iii*) use these complexes to investigate reaction pathways involved in the catalytic cycle characteristic for hydroaminations. These results provide direct evidence that the general difficulty associated with hydroamination of alkenes does not originate in the thermodynamic binding differences, but rather in an uncompetitive protodeauration step.

[a] *J. Gubler,[+] M. Radić,[+] Y. Stöferle, P. Chen*
Laboratorium für Organische Chemie
ETH Zürich
Rämistrasse 101, 8092 Zürich (Switzerland)
E-mail: peter.chen@org.chem.ethz.ch

[+] *These authors contributed equally to the publication.*

Supporting information for this article is available on the WWW under https://doi.org/10.1002/chem.202200332

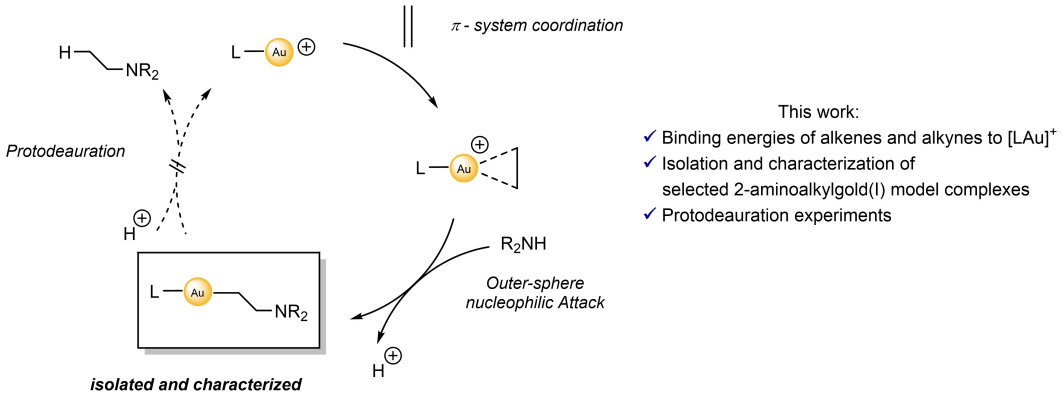

Scheme 1. A hypothetical catalytic cycle for an outer-sphere hydroamination of alkenes.

Results

Binding energies of alkenes and alkynes

Trimethylphosphine gold(I)-complexes of terminal and internal octenes and octynes were prepared in the gas phase by electrospraying 40 μM solutions of $[(Me_3P)Au(MeCN)][SbF_6]$ from methanol followed by thermalization with corresponding unsaturated substrates at 0.2 mbar, and investigated by mass spectrometry. The specially modified electrospray ionization tandem mass spectrometer (ESI-MS/MS), the measurement procedures, and the L–CID program for deconvoluting the experimental threshold energy, $E_{0,exp}$, from the threshold collision-induced dissociation (T-CID) data, have been described previously.[8,9] Specifically for the present instance, the threshold energies, $E_{0,exp.}$, pertaining to the dissociation of unsaturated hydrocarbons from adducts containing *trans*-4-octene, 1-octene, 1-octyne and 4-octyne were measured, the errors estimated and the values compared with those stemming from computations and from a previous report by Roithová and coworkers for similar systems.[10]

The results of the measurements are shown in Table 1 and allow for several observations. Dissociation energies of complexes of 1-octene and 1-octyne are experimentally indistinguishable, indicating that no intrinsic binding preference of $[(Me_3P)Au]^+$ towards 1-octyne exists, when compared to the corresponding alkene, 1-octene. 4-Octyne, an internal alkyne, binds more strongly than its terminal isomer, whereas *trans*-4-octene binds more weakly. Considering the associated errors, we note that the magnitudes of binding energies are reproduced reasonably well by DFT calculations at the PBE0/cc-pVTZ level of theory, at least for the limited set of structures for which we report experimental data. This justifies the usage of this level of approximation for computational studies in our work.

Table 1. Comparison between the experimental threshold energies, $E_{0,exp}$, of alkene and alkyne dissociation from $[(Me_3P)Au(alkene)]^+$ and $[(Me_3P)Au(alkyne)]^+$ complexes, determined via CID, and energies obtained by DFT calculations, PBE0-D3(BJ)/cc-pVTZ//PBE0/cc-pVTZ. Experimental errors are determined by the degree of reproducibility, as well as an error analysis of the L–CID model.[11]

Unsaturated hydrocarbon	$E_{0,exp.}$	E_{DFT-D3}	ΔE
	[kJ/mol] [kcal/mol]	[kJ/mol] [kcal/mol]	[kJ/mol] [kcal/mol]
trans-4-octene	186.2 ± 4.2	197.9	11.7
	44.5 ± 1.0	47.3	2.8
1-octene	196.2 ± 4.2	189.5	−6.7
	46.9 ± 1.0	45.3	−1.6
1-octyne	196.2 ± 4.2	191.6	−4.6
	46.9 ± 1.0	45.8	−1.1
4-octyne	207.9 ± 4.2	210.5	2.5
	49.7 ± 1.0	50.3	0.6

Synthesis of 2-aminoalkylgold(I) complexes and their reactivity in solution

We further report a method for the preparation of 2-aminoalkyl gold(I) complexes, which would be the putative intermediates in either the inner-sphere or outer-sphere mechanism for the alkene hydroamination. The preparation is possible by means of nucleophilic substitution of the chloride ligand of [LAuCl] complexes (where L = IPr, IPr^{Me}, JohnPhos, XPhos) with an appropriate C-nucleophile obtained by deprotonation. Considering that this would necessitate deprotonation of the β-position of the amine, which is intrinsically not very acidic, we found that stabilization of the negative charge by an adjacent phenyl group was required. However, phenylethylamine substrates are prone to β-elimination under the conditions for deprotonation, which made the synthesis challenging. To circumvent the problem of β-elimination, the method presented here relies on the report by Strohmann et al., who disclosed successful β-deprotonation and functionalization of (2-phenylethyl)dimethylamine using Schlosser's base.[12] They describe the vital role of potassium as a counterion, which renders the intermediate structure more stable against β-elimination.

Specifically, despite various solvents and additives having been investigated, widely used lithiation reagents, *n*-BuLi and *t*-BuLi, are either unable to deprotonate (2-phenylethyl)-dimethylamine at all, or they lead to its degradation via elimination of

dimethyl amine. Strohmann et al. showed that quantitative deprotonation is possible with either the mixture consisting of *t*-BuLi and KO*t*-Bu (1 equiv. / 1 equiv.) or *n*-BuLi and KO*t*-Bu (2 equiv. / 2 equiv.).

Upon treatment of [LAuCl] complexes containing different dialkylbiaryl phosphine- and NHC- ligands with the metalated (2-phenylethyl)dimethylamine nucleophile, obtained by the abovementioned method, we were pleased to observe that the transmetalation took place and that the desired 2-aminoalkyl gold complexes were formed. While optimizing the reaction conditions, we successfully implemented both deprotonation methods mentioned above.

We selected the two group representatives, [(JohnPhos)Au{CH(Ph)CH_2NMe_2}] and [(IPr)Au{CH(Ph)CH_2NMe_2}] for further studies.

Strohmann's report addresses the issue of the problematic deprotonation of a single substrate, that of (2-phenylethyl)dimethylamine. We prepared a series of derivatives of this compound, and tested the influence of modification of aryl group, alkyl chain and amine substituents on the metalation (Scheme 2). While we use only a selected subset of the prepared compounds for the mechanistic studies, the scope of the synthesis, and the characterization of the broader set of compounds are presented in greater detail in the Supporting Information: Section 2.3.

With the 2-aminoalkyl gold(I)-complexes at hand, we performed solution NMR experiments which aimed to investigate the protodeauration step. [(JohnPhos)Au{CH(Ph)CH_2NMe_2}] was titrated with diluted triflic acid (TFA) in THF-d_8 at room temperature. We observed no (2-phenylethyl)-dimethylamine, which would have been the product of a protodeauration. Rather, the product of the clean reaction could be identified as free styrene, indicating that an elimination of the amine had taken place.

The reaction proceeded cleanly upon incremental addition of 0.25 equiv. of triflic acid up until 1.0 equiv., at which point the NMR spectra indicated quantitative and exclusive conversion of the starting complex to styrene. Further addition of 0.5 equiv. of triflic acid until 2.0 equiv. resulted in no further change in the styrene concentration, as expected (Figure 1a). Peak (P) could be assigned to the 6 H-atoms of the methyl groups of product species and it shows interesting behavior: below 1 equiv. of triflic acid, peak P was broadened and there was a gradual downfield shift following incremental addition of 0.25 equiv. of triflic acid. Assuming an exchange process of the free dimethylamine with gold-bound species, we treated the starting material complex, [(JohnPhos)Au{CH(Ph)CH_2NMe_2}], with 0.5 equiv. TfOH and studied dynamics by NMR at variable temperatures (for spectra see the Supporting Information: Section 5.2.2). As expected, at −80 °C splitting of the broad peak at 2.37 ppm was observed, resulting, among others, in a peak at 2.29 ppm. This matches very well with the methyl signal at 2.27 ppm in the separately recorded ^{1}H NMR spectrum of free dimethylamine in THF-d_8 at room temperature. Downfield shift of the averaged peak, observed upon increase in triflic acid equivalents, cannot, however, be explained by a single exchange process, as the additional triflic acid would simply result in the increase in concentration of the products, but their ratio would be the same, as governed by the equilibrium constant. This implies the involvement of other species in the exchange. Indeed, we were able to observe this in our ^{31}P and ^{1}H NMR spectra. The details on the speciation and the corresponding spectra are given in the Supporting Information: Section 5.2.2. The second distinguishable stage of the titration was reached when excess triflic acid was added. This led to the protonation of dimethylamine, resulting in the 6 H-atoms of the methyl groups being split up to a triplet (T) by two neighboring protons in $Me_2NH_2^+$, as seen in Figure 1b. The ^{1}H NMR signal at 2.47 ppm (dd, ^3J (H,H) = 5.9 Hz and ^4J (P,H) = 1.8 Hz), as well as ^{31}P signal at 57.1 ppm of the product complex could also be related to those reported for [(JohnPhos)Au(NEt_2H)]SbF_6.

In a second experiment, [(IPr)Au{CH(Ph)CH_2NMe_2}] was likewise titrated with triflic acid in THF-d_8, once again resulting in the formation of free styrene and [(IPr)Au(NMe_2H)]OTf.

Interested whether the outcome of the protonation is dependent on the acid employed, we conducted the reaction using different Brønsted acids. The reaction proceeded with AcOH, reaching completion at 1.1 equiv. of AcOH, as well as with 12 equiv. of phenol. There was no observable reaction when 1 equiv. of phenol or 110 equiv. of methanol were used.

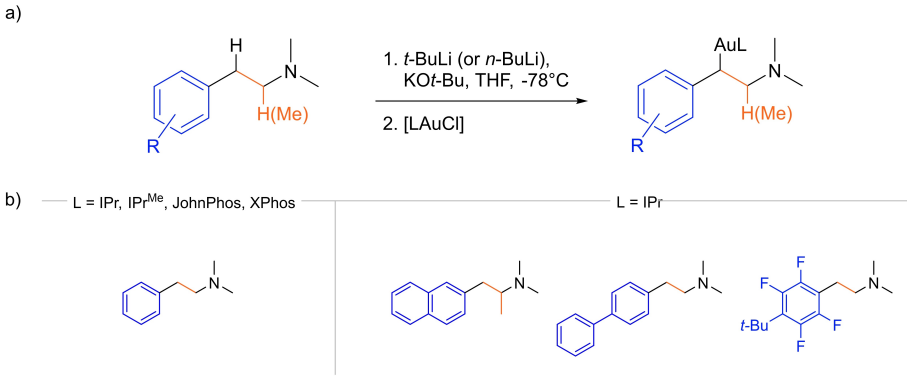

Scheme 2. a) Synthesis of 2-aminoalkyl gold(I) complexes, and b) scope of 2-arylethan-1-amines, which successfully underwent both LICKOR metalation and auration. The first step, LICKOR-metalation was decisive for the success of the overall reaction. The second step, auration, was possible for a range of ligands. For other investigated ligands and substrates see the Supporting Information: Sections 2.2 and Section 2.3.

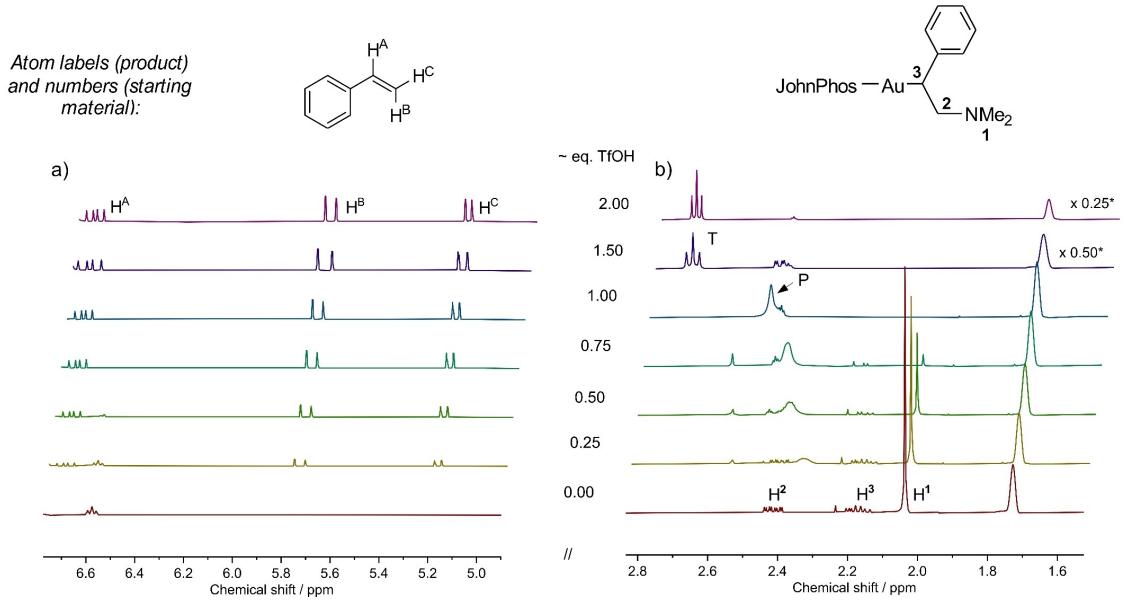

Figure 1. ^{1}H NMR titration of [(JohnPhos)Au{CH(Ph)CH$_2$NMe$_2$}] by using triflic acid in THF-d_8. a) Diagnostic peaks showing the formation of styrene. b) Diagnostic peaks showing the disappearance of the starting material (H^1, H^2, H^3) and formation of the product (P) and the ammonium salt of the secondary amine (T). * Intensities of the spectra at 1.50 and 2.00 equiv. were scaled by 0.5 and 0.25, respectively. Apart from peaks due to THF and internal standard, there are no peaks of relevance between 2.8 and 5.0 ppm. Full spectra can be found in the Supporting Information: Section 5.2.1.

This comes without surprise when one considers the pK_a differences of protonated tertiary amines (e.g. triethylammonium ion, pK_a = 10.7 in H_2O)[13] and pK_a of methanol (pK_a = 15.5 in H_2O).[14] A model calculation finds that protonation of 50% of (2-phenylethyl)dimethylamine present in the solution at comparable concentrations as those used in the titration (31.6 μmol/ml), would require ca. 3000 equivalents MeOH. In DMSO, differences in pK_a are considerably larger (ΔpK_a = 20) than in H_2O, bringing about negligible protonation. Importantly, in all the cases where the reaction did proceed at all, we observed styrene as the product.

Analogous experiments were performed using different Lewis acidic methylating agents instead of Brønsted acids. [(JohnPhos)Au{CH(Ph)CH$_2$NMe$_2$}] was treated with methyl iodide and methyl *p*-toluenesulfonate in C_6D_5Cl at room temperature. NMR analysis showed that a full conversion of the gold complex took place, with styrene being formed within less than 10 min. Further, following the treatment of [(IPr)Au{CH(Ph)CH$_2$NMe$_2$}] with 1.3 equiv. of methyl triflate in CD_2Cl_2 at −80 °C, an even stronger methylating agent, a ^{1}H NMR measured after 3 min showed again the full conversion of the gold complex and formation of styrene, [(IPr)Au(NMe$_3$)]OTf and (Me_4N)OTf. A ^{19}F NMR signal at -74.8 ppm indicated the presence of unreacted methyl triflate, besides the signal at −79.4 ppm assigned to [(IPr)Au(NMe$_3$)]OTf and [Me_4N]OTf. NMR spectra of the protonation and methylation experiments can be seen in the Supporting Information: Section 5.

As will be seen in the Discussion, the Results with respect to the solution reactivity of the protonated [(JohnPhos)Au{CH(Ph)CH$_2$NMe$_2$}] are the most important observations in this study.

ESI-MS/MS of protonated 2-aminoalkyl gold complexes

Dilute solutions of 2-aminoalkyl gold complex [(IPr)Au{CH(Ph)CH$_2$NMe$_2$}] in 1,2-dichloroethane were introduced into the mass spectrometer by electrospray ionization (ESI). A weak signal appeared at *m/z* 734, where the protonated adduct ion $[MH]^+$ would be expected. However, products of amine elimination $[(IPr)Au(styrene)]^+$ and $[(IPr)Au(NMe_2H)]^+$, as well as dinuclear complexes $[(IPr)_2Au_2Cl]^+$ and $[(IPr)_2Au_2(C_{10}H_{14}N)]^+$ were more abundant in the mass spectrum, indicating that elimination was already occurring during the electrospray process, either in solution or in the gas phase. This spectrum and spectra in other solvents are included in the Supporting Information: Section 3.1. The microscopic reverse of an outer-sphere addition produces a cationic styrene complex, which we would see in the mass spectrum, and a neutral amine, which is invisible to mass spectrometry. In the mass spectrum, the abundance of styrene complex ions was much higher than that of amine complex ions, and, therefore one may conclude that there is hardly any ligand substitution of styrene for amine. An amine complex formed thereby, would have been more stable[4,15] (see the Supporting Information: Section 2.5), as amines typically bind more strongly to $[LAu]^+$ than olefins or alkynes. Hence either elimination occurred in solution and there was not enough time for ligand exchange with the amine, or elimination took place in the gas phase, where the amine loss is irreversible.

While, as mentioned above, the signal for the ion with the mass-to-charge ratio of a 2-ammoniumalkyl gold complex, $[MH]^+$, at m/z 734, was weak, it could nevertheless be selected and subjected to collision induced dissociation (CID, Figure 2

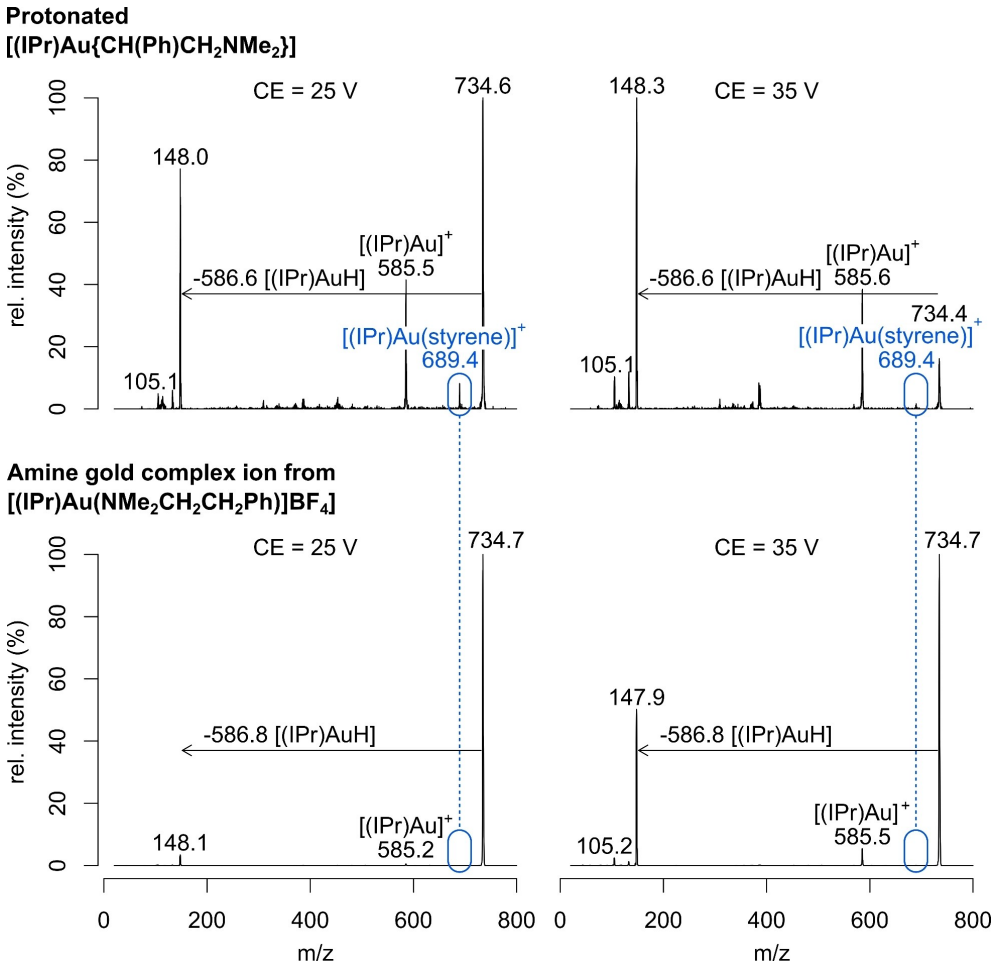

Figure 2. Comparison of the collision-induced dissociation (CID) mass spectra for protonated 2-aminoalkyl gold complex ions (top) and 2-(phenylethyl)dimethylamine gold complex ions (bottom). CID parameters: collision energy (CE) 25 V (left) or 35 V (right) in the lab frame, collision pressure = 0.5 mTorr argon.

top), upon which it mainly fragmented to fragment ions at *m/z* 585 $[(IPr)Au]^+$ and *m/z* 148 ($C_{10}H_{14}N^+$). The fragment ion signal at *m/z* 689, assigned to $[(IPr)Au(styrene)]^+$, was weak, but reproducibly observable, especially at the lower collision energies. A hypothetical protodeauration could possibly lead to a rearrangement to the gold amine complex ions of type $[(IPr)Au\{N(Me_2)CH_2CH_2Ph\}]^+$ with m/z 734, which would have the same mass as $[(IPr)Au\{CH(Ph)CH_2NHMe_2\}]^+$, the 2-ammonium alkyl gold complex, $[MH]^+$, as indicated in Scheme 3. We sought to distinguish between $[(IPr)Au\{CH(Ph)CH_2NHMe_2\}]^+$ and the isomeric $[(IPr)Au\{N(Me_2)CH_2CH_2Ph\}]^+$ by differences in their CID behavior. We prepared an authentic sample of the alternative structure by reaction of $[(IPr)Au(CH_3CN)]BF_4$ and (2-phenylethyl)dimethylamine. A THF solution of the isolated authentic alternative amine complex, $[(IPr)Au\{N(Me_2)CH_2CH_2Ph\}]^+$, was electrosprayed. The CID spectra of protonated adduct ions $[MH]^+$ and authentic amine complex ions were similar, the latter needing higher collision energies for significant fragmentation at all, but importantly differing in the absence of $[(IPr)Au(styrene)]^+$, m/z 689, at any collision energy. While we cannot exclude definitively that part of the signal at *m/z* 734 derives from the alternative amine complex, we conclude that a significant fraction of the signal at m/z 734 comes from the desired $[MH]^+$ that survived the electrospray.

Other than for the complexes with IPr, CID spectra of protonated adduct ions were also compared with amine complexes for a range of other ancillary ligands, i.e., phosphite $(2,4\text{-}t\text{-}Bu_2C_6H_3O)_3P$ and phosphines Me_3P, $t\text{-}Bu_3P$, Ph_3P and JohnPhos. Only for the protonated 2-aminoalkyl gold(I) complex ions with Me_3P did we also see styrene complex fragment ions. For the other ligands the presence of this particularly diagnostic fragment could not be detected (see the Supporting Information: Section 3.1.3).

Fragments at *m/z* 148 ($C_{10}H_{14}N^+$), which are present in the CID of complex ions with all ligands except JohnPhos, are likely formed through loss of a gold hydride [(L)AuH]. Gold complex ions of structurally simpler tertiary amines, for example $[(IPr)Au(NEt_3)]^+$, underwent a similar fragmentation (see the Supporting Information: Section 3.3). To identify the origin of the hydride, the 2-aminoethyl gold complex $[(IPr)Au\{CH(Ph)CH_2NMe_2\}]$ was labeled with deuterium in different positions. When the methylene group was selectively monodeuterated, the complex ion lost [(IPr)Au(H)] as well as [(IPr)Au(D)] (Scheme 4). The products therefore correspond to those of a β-hydride elimination

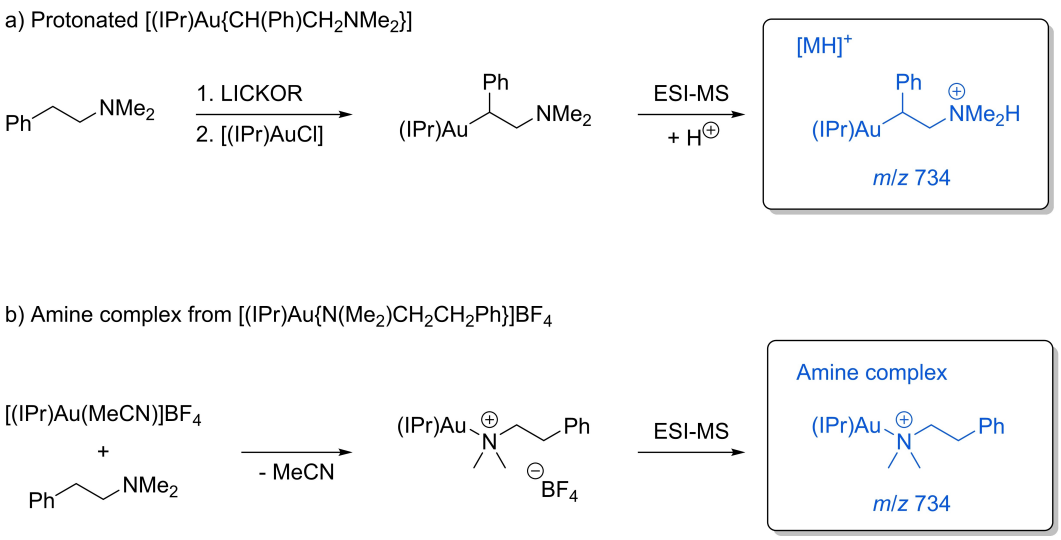

Scheme 3. Preparation of precursors and ESI-MS of the protonated adduct ions $[MH]^+$ and authentic amine complex ions. Both complex ions have identical elemental composition $[C_{37}H_{51}N_3Au]^+$ and are isomeric.

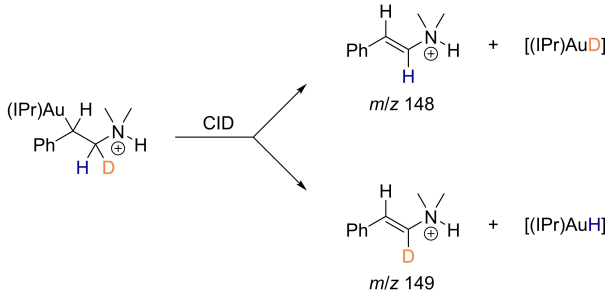

Scheme 4. CID fragmentation of the 2-amino(2-^{2}H)alkyl gold complex. Spectra are given in the Supporting Information: Section 3.1.4.

producing an enammonium ion. The mechanistic nature of the process however need not be that of a conventional β-hydride elimination (see below). Further labeling experiments demonstrated that the hydrons and the methyl groups of the ammonium group can be excluded as source of the hydride.

ESI-MS/MS of methylated 2-aminoalkyl gold complexes

Methylation of the amino group in $[(IPr)Au\{CH(Ph)CH_2NMe_2\}]$ produces a 2-trimethylammoniumalkyl gold complex that cannot protodeaurate intramolecularly like its protonated analog presumably could have. This gives us the opportunity to investigate exclusively elimination. With methyl triflate, $[(IPr)Au(NMe_3)]OTf$ was formed rapidly in solution (see NMR experiments above), and in the simplest mechanism (*lex parsimoniae*), methylation occurs directly on the nitrogen and not on the carbon or gold atom. The unstable ammonium alkyl gold complex was observed in the mass spectrum when an inline flow reactor was directly coupled to the ESI source (contact time 0.7 min, see the Supporting Information: Section 3.2). We were pleasantly surprised to see the olefin complex ions occurring more abundantly in the CID spectrum of $[(IPr)Au\{CH(Ph)CH_2NMe_3\}]^+$, as seen in Figure 3, than they did for the protonated adduct ions in Figure 2. Unexpectedly, there was no loss of [(IPr)AuH] anymore (see the Supporting Information: Section 3.2.2). CID spectra for different 2-trimethylammoniumalkyl gold(I) complex ions were also recorded (see the Supporting Information: Table S7). The amount of olefin complex ions from fragmentation ranged from none to dominant.

While the solvation may be expected to influence the potential energy surface for ionic reactions significantly, we point out that, of the three gas-phase reactions seen in the ESI-MS/MS spectra of either the protonated or methylated 2-aminoalkylgold(I) complexes, two product channels, formation of $[(L)Au(olefin)]^+$ and $[(L)Au]^+$ ions, are, in fact, consistent with amine elimination, with or without subsequent loss of olefin, that we observed in solution. The third product channel, i.e. formal β-H elimination, appears to be unique to the gas phase and provides little information on the chemistry in solution. A combined computational and experimental study by Hashmi, Köppel et al. showed explicitly that the β-hydride elimination in NHC- and phosphine-alkylgold(I) complexes constitutes a highly unlikely elementary step in solution. DFT calculations predicted high barriers for the β-hydride elimination, further enabling estimation of rate constants by classical transition state theory. Solution experiments were conducted by measuring decomposition temperatures of different alkylgold(I) complexes: No β-hydride elimination products could be detected. The complexes rather underwent other decomposition pathways below the high temperatures predicted necessary by DFT modelling for a β-hydride elimination.[16] Therefore, the observed product channel can be more properly understood as a reaction within an electrostatically-bound ion-neutral complex (INC), for which similar reactions are known in the mass spectrometric literature.[17–19] All three channels for the gas phase CID, but

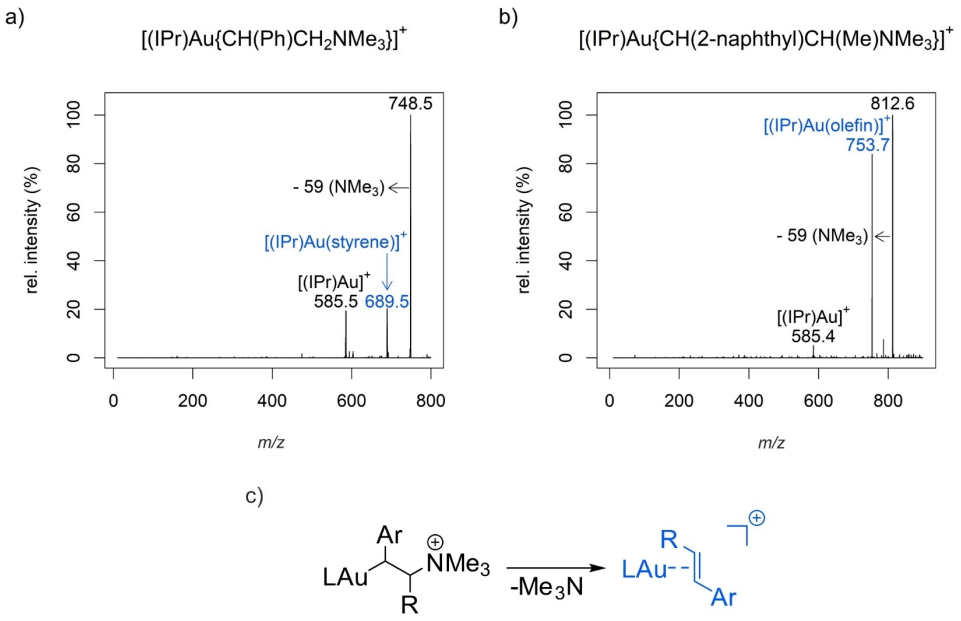

Figure 3. a) CID mass spectra of $[(IPr)Au\{CH(Ph)CH_2NMe_3\}]^+$ and b) $[(IPr)Au\{CH(2\text{-}naphthyl)CH(Me)NMe_3\}]^+$. Fragmentation to the olefin complex ion is a prominent channel for the former, and the dominant channel for the latter. c) Presumed fragmentation pathway. CID parameters: collision energy 20 V (a) / 15 V (b), collision pressure = 0.5 mTorr argon.

especially the third, are discussed in the Supporting Information: Section 3.4.

Discussion

The efforts invested in the development of various hydrofunctionalization reactions are a response to the general need for efficient processes generating carbon-heteroatom bonds. Because of their theoretically perfect atom economy, hydrofunctionalizations are considered one of the key approaches to this problem. The scope of the reactions contained in this term is very broad and different levels of success were achieved for different functional groups. However conceptually simple, hydroamination of alkenes, essentially ergoneutral, nevertheless does not proceed on its own. Reasonable rates in the reaction require the involvement of catalysis.

In particular, hydroaminations catalyzed by gold(I) require additional and unique considerations. Relativistic effects are known to influence the reactivity of heavy elements in general, and are particularly pronounced for gold.[20,21] Further, $[LAu]^+$ fragments are isolobal[22] to H^+ which means that, for those steps of the catalytic cycle where protonation is assumed, auration represents a possible alternative, and vice versa, at least in principle. Of particular relevance to understanding our subsequent Discussion, 2-aminoalkyl gold complexes, which are in the focus of this report, could react with $[LAu]^+$, in principle, forming gem-diaurated species. Analogous gem-diaurated intermediates are documented in the literature,[23] and we will use the isolobal analogy to rationalize some of our results. It has also been generally observed that, whereas hydroamination of alkynes proceeds readily, alkenes are much more difficult substrates. Notable progress has been made through the work of He et al., who disclosed an intermolecular addition of sulfonamides to unactivated alkenes using $[(Ph_3P)AuCl]$ and an intermolecular addition of synthetically relevant Cbz-type sulfonamides to 1,3-dienes enabled by $[(Ph_3P)AuOTf]$.[24,25] In this report, we do not seek to address all the open mechanistic question concerning hydroamination of π-systems, but rather we provide an answer to the specific question of why alkenes do not undergo successful gold catalyzed hydroamination reactions when compared to alkynes.

To account for the apparent chemoselectivity of gold(I) complexes towards alkynes when compared to alkenes, several research groups have investigated the binding affinity argument, which claims that gold(I) binds stronger to alkynes than alkenes. Roithová et al. used threshold collision-induced dissociation (T-CID) mass spectrometry to determine the binding energies of $[Au(PMe_3)]^+$-cations to different alkenes and alkynes.[10] Upon T-CID using xenon gas, the products of the dissociation event were largely unsaturated hydrocarbons, accompanied with minor formation of trimethylphosphine. In the series of 1-pentene, 1-pentyne and 2-pentyne adducts, threshold energies of 175.6 ± 4.8 (42.0 ± 1.2), 181.4 ± 6.8 (43.4 ± 1.6), 184.3 ± 3.9 (44.0 ± 0.9) kJ/mol (kcal/mol) were reported, respectively. For adducts of styrene and phenylacetylene energies of 178.5 ± 3.9 (42.7 ± 0.9) and 180.4 ± 3.9 (43.1 ± 0.9) kJ/mol (kcal/mol) were documented, respectively. Furthermore, based on computational and ligand exchange studies, they showed that ethylene binds the cation more strongly than acetylene, but more weakly than propyne. This indicates that the differences due to substitution within a compound class, alkynes in this case, exceed the differences between different compound classes, that of alkenes and alkynes - a point also

made by Widenhoefer in his solution NMR experiments (see below). As noted by Roithová et al., lack of proper thermalization potentially underestimates the binding energies. Nevertheless, the relative order of energies reported by Roithová et al. is correct in our view.

Along these lines, Widenhoefer used NMR measurements to determine solution binding affinities of alkenes and alkynes (unsaturated hydrocarbons, UHC) for the $[(JohnPhos)Au]^+$ fragment.[26] Specifically, equilibrium constants (K) for the $NCAr_F$ ($NCAr_F = N{\equiv}C\text{-}3,5\text{-}C_6H_3(CF_3)_2$) ligand displacement as depicted in Scheme 5 were determined, and the binding affinities inferred from them.

The reaction was performed in CD_2Cl_2 at −60 °C, resulting in the following values of K for the series of UHCs with 6 C-atoms: 133 ± 10, 86 ± 7, 450 ± 39 for 1-hexene, 2-hexyne and 3-hexyne respectively. Furthermore, K was found to be 25 ± 2, 14.1 ± 0.4 for 2-butyne and *trans*-butene, respectively. Hence, while 2-hexyne exhibits weaker binding than 1-hexene, its isomer, 3-hexyne, binds more strongly.

Having a reliable protocol for the gas-phase bond dissociation energy determination using T-CID mass spectrometry at our disposal,[8,9] we have decided to revisit the issue of binding energies of alkenes and alkynes. The results presented in the Table 1 show that there is no statistically significant difference in the binding energies between 1-octene and 1-octyne. While *trans*-4-octene does bind less strongly than 4-octyne, our data are consistent with the observations presented by Roithová[10] that the difference in binding energy between members of the same class, alkenes vs. alkenes or alkynes vs. alkynes, is comparable to the difference between members of different classes. While binding energies in the gas phase may be difficult to compare to free energies of binding in solution (which include entropy), Widenhofer's equilibrium constants, measured at low temperature where $T\Delta S$ is reduced, give the same overall conclusion that binding energies cannot be the principal reason for the systematically different behavior of alkenes vs. alkynes in Au(I)-catalyzed hydroamination reactions.

Based on the results presented above, we find ourselves again confronting the question of the privileged status of alkynes in the hydroamination reactions. We hypothesize that the origin of the difference lies in the protodeauration step, which is outcompeted by an elimination pathway leading back to the alkene starting material. This was, in fact, previously suggested by Toste et al. for a specific case of intramolecular amidoauration of alkenes, as well as Fürstner in his insightful review.[27,28] Our synthesis of the key 2-aminoalkyl gold(I) complexes, which correspond to the putative intermediates in the catalytic cycle, offers us the opportunity to test this hypothesis directly for the more general case of the intermolecular hydroamination reaction of alkenes.

In what we recognize to be the most important experiment we report, protonation of a THF solution of independently synthesized $[(JohnPhos)Au\{CH(Ph)CH_2NMe_2\}]$, a model for the putative intermediate after nucleophilic attack by the amine in the outer-sphere mechanism, resulted in quantitative formation of styrene and the gold amine complex. This direct experiment demonstrates that protodeauration (forward in catalytic cycle) is not kinetically competitive with elimination (backward in the catalytic cycle).

Markovnikov selectivity, as discussed in the context of Brønsted acid-catalyzed addition reactions of unsymmetric alkenes, is primarily of thermodynamic nature and arises from the energetic difference between discrete reaction intermediates generated in the rate-determining protonation step (this with the exception of those reactions where considerations involving non-classical carbocations are necessary). Most commonly the mentioned intermediates are carbocations with a different substitution level. The subsequent step, nucleophilic addition, proceeds from two distinct intermediates in two competing pathways. In the case of gold(I)-catalyzed hydrofunctionalizations, a single intermediate preceding nucleophilic attack is in general assumed, namely a gold(I)-π system complex. This means that the regioselectivity-determining step takes place after the coordination of gold(I), as opposed to the case of the proton-catalyzed reactions. We can then judge whether our 2-aminoalkyl gold complexes, which result from a formal *anti*-Markovnikov addition, are adequate models for the protodeauration of a Markovnikov intermediate. It should be sufficient to compare the differences between the elimination and protodeauration barriers of the Markovnikov intermediate with those obtained from the *anti*-Markovnikov intermediate. Calculations at the PBE0-D3(BJ)/def2-TZVP level of theory using the SMD (Solvent Model Density) solvent model reproduced our NMR solution results well enough. Employing these calculations, the Markovnikov intermediate, $[(IPr)Au\{CH_2(NHMe_2)CHPh\}]^+$, was located 26.4 kJ/mol (6.3 kcal/mol) above the *anti*-Markovnikov intermediate, $[(IPr)Au\{CH(Ph)CH_2NHMe_2\}]^+$. The protodeauration transition state along the Markovnikov pathway was found to lie 33.0 kJ/mol (7.9 kcal/mol) higher, and the elimination transition state 2.9 kJ/mol (0.7 kcal/mol) lower than their *anti*-Markovnikov counterparts (Figure 4). Therefore, if the nucleophilic addition does

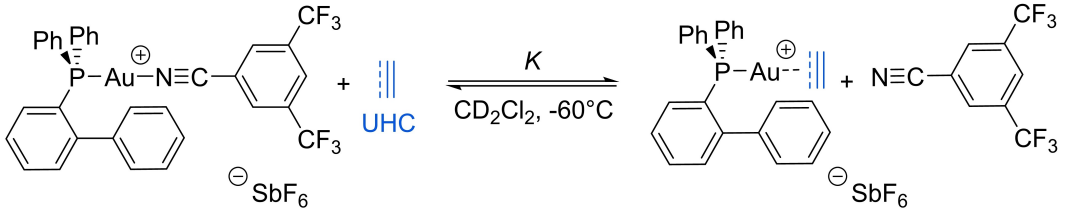

Scheme 5. Equilibrium showing the exchange of the $NCAr_F$ ligand with the unsaturated hydrocarbon examined by Widenhoefer et al. in their solution NMR studies.[26]

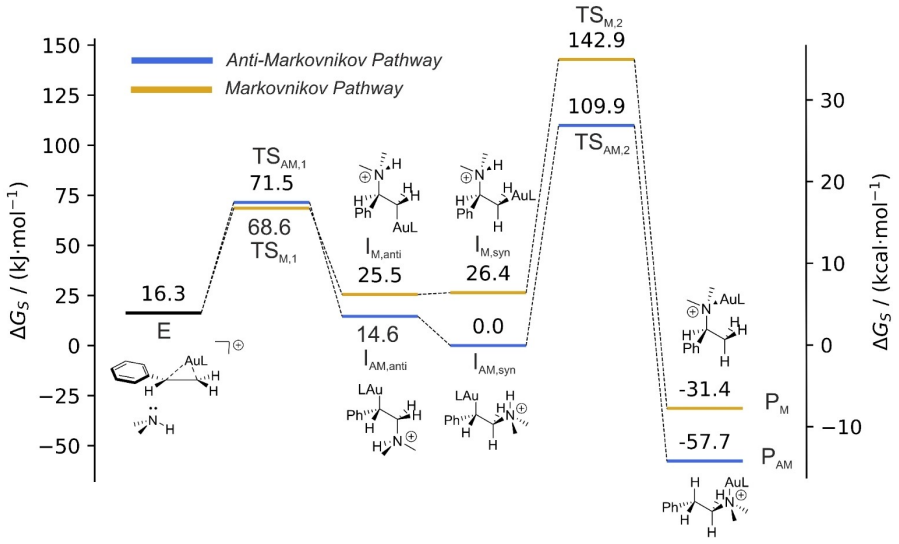

Figure 4. Relative standard state-corrected solution Gibbs free energies for the studied *anti*-Markovnikov and Markovnikov additions of Me_2NH to [IPrAu(styrene)], as obtained at the PBE0 D3(BJ)/def2-TZVP SMD level of approximation. $I_{AM,}$ $TS_{AM,1}$, $TS_{AM,2}$ and P_{AM} represent the protonated 2-aminoalkylgold(I) intermediate, the transition state of the elimination pathway, the transition state of the protodeauration step and the product of the anti-Markovnikov pathway, respectively. $I_{M,}$ $TS_{M,1}$, $TS_{M,2}$ and P_M are to be interpreted analogously for the Markovnikov selectivity. E is the sum of energies of infinitely separated $[(IPr)Au(styrene)]^+$ and Me_2NH. Elimination reaction was assumed to proceed from the Au–C–C–N *anti*-conformer and protodeauration from an Au–C–C–N *syn*-conformer of the corresponding protonated 2-aminoalkylgold(I) intermediates.

proceed to a Markovnikov intermediate, the protodeauration step would be even slower and elimination even faster than in the *anti*-Markovnikov case (Details can be found in the Supporting Information). With protodeauration as the rate-determining step, the selectivity is no longer governed by simple considerations of energetic differences in barriers of the nucleophilic attack. Stated differently, the nucleophilic addition is a pre-equilibrium to the rate-determining protodeauration. General problems associated with the computations involving implicit solvent models, especially when these are used for bimolecular ionic reactions involving organometallic systems mean that we limit ourselves to this qualitative comparison. The differences are large enough that we consider the conclusion to be reliable, hence we do not further address the selectivity in detail. Accordingly, while most gold(I) catalyzed hydrofunctionalizations occur with Markovnikov selectivity and therefore might produce $[(IPr)Au\{CH_2(NHMe_2)CHPh\}]^+$, a regioisomer to the 2-aminoalkyl gold complex we were able to prepare, we expect that our formally anti-Markovnikov regioisomer also presents an adequate model for the intermediate of Markovnikov addition.

Having established experimentally that protonation or alkylation of a 2-aminoalkyl gold(I) complex triggers amine loss exclusively in solution, and noticeably-to-predominantly in the gas phase, we have made an observation which explains why the catalytic cycle for Au-catalyzed hydroamination does not turn over for alkenes. Going beyond the phenomenon itself to ascertain *why* protodeauration does not compete with amine elimination, we need to consider the possible transition state(s) for protodeauration.

For our 2-aminoalkyl gold complexes, we consider, *a priori*, three different mechanisms for protodeauration, shown in Scheme 6: *(i)* direct electrophilic attack (3-center S_E2) of H^+ at the Au–C bond (*M1*), *(ii)* protonation of nitrogen followed by intramolecular H^+ transfer (*M2*), and *(iii)* protonation of the metal followed by intramolecular H^+ transfer ($S_E$ox, *M3*). Treatment of protonations by quantum chemical methods is challenging because solvation is especially important for charged species.[29] Furthermore, the electronic structure of the reactant can change considerably upon reaction with a proton,[30] and therefore the reactivity descriptors that are based on the electronic structure of the reactant may not always be predictive (see the Supporting Information: Section 6.3 on NBO energies). We therefore decided to base our following Discussion on experimental precedents for related systems whenever possible, using quantum chemical methods only to study relative energies between isomers, and to search for possible intermediates. In other words, the quantum chemical calculations should be regarded rather as permissive than definitive, giving us only a qualitative to semi-quantitative (at best) picture.

We discuss each of the three mechanisms individually, and then indicate what all three have in common.

Mechanism 1: Direct electrophilic attack on the Au-C σ-bond

Alkylgold complexes [LAuR] are isoelectronic to dialkylmercury(II) compounds [RHgR']. For the protonolysis of the latter, a frontside 3-center electrophilic attack (S_E2, cf. TS-M1) had been proposed to explain the high H/D kinetic isotope effect of 9–11 and retention of configuration of the carbon atom.[31] Ultraviolet photoelectron spectroscopy on $[(Me_3P)AuCH_3]$ in the gas phase identified the σ(Au,C)-bonding

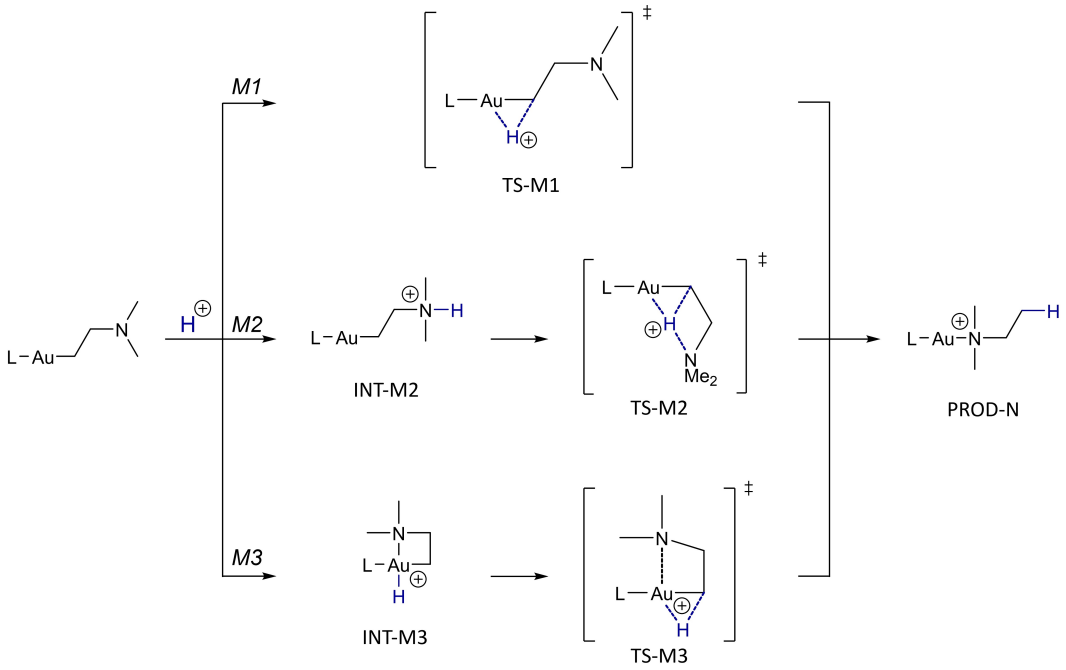

Scheme 6. Truncated transition states (TS), intermediates (INT) and product (PROD) for protodeauration mechanisms *M1*, *M2*, and *M3*. In INT-M3 the nitrogen completes the coordination sphere of the Au(III) center. A systematic DFT search identified other stable protonated species, however, these were much higher in energy and judged not to be considered relevant (Supporting Information: Section 6.4).

orbital as the HOMO.[32] Under frontier orbital control, this would be the orbital that interacts with the LUMO of the electrophile most strongly. Monoligated coinage metal complexes (LM^+, where M=Cu, Ag or Au) are isolobal to H^+, however, they are more polarizable and therefore softer in the HSAB concept. This favors frontier (orbital) control over charge control and should make soft transition metal electrophiles better probes for the HOMO than H^+.[33] Indeed, XRD structures have been reported where monoligated coinage metal complexes ($[LM^+]$) bind to metal-carbon σ-bonds.[34] For H^+ no analogous structures have been reported, as far as we know, and we therefore consider these structures to be transition states for protonation (TS-M1). An ion with the mass-to-charge ratio of protonated dimethyl mercury ($HgMe_2H^+$) had been observed by mass spectrometry, but its structure was not determined.[35] The analogy to Hg(II) and the nature of the HOMO identify direct electrophilic attack on the Au–C σ-bond as a plausible mechanism, in principle. We will argue, however, that this is unlikely for the protonation of {(L)Au[CH(Ph)CH_2NMe_2]} (see below).

Mechanism 2: Protonation of the amine nitrogen

N-protonation of 2-aminoalkyl gold complexes forms the bound ammonium species (INT-M2). The pK_a of the conjugate acid of tertiary aliphatic amines was estimated to be around 12.7 in THF.[36] Consequently, *N*-protonation of 2-aminoalkyl gold complexes by moderate to strong acids, like HOTf, protonated THF or HOAc, should be thermodynamically favorable. Furthermore, qualitative models like the HSAB concept or reorganization theories by Eigen, Marcus and others,[37–40] predict *N*-protonation to be fast compared to protonation of the α-carbon. In line with this reasoning, kinetic protonation was selective for the nitrogen over the unsaturated α-carbon in enamines.[41,42] We therefore expect *N*-protonation to be kinetically and thermodynamically favorable for our 2-aminoalkyl gold complex as well. If the triflate anion were the only base in the system, the equilibrium concentration of unprotonated 2-aminoalkyl gold complex would be virtually zero, but other bases are present, for instance THF itself, making the concentration non-zero. With fast and reversible *N*-protonation as a pre-equilibrium for protodeauration, mechanism *M2* would correspond to the case of specific acid catalysis, in this case, of a protodeauration reaction.

In titrations of [(L)Au{CH(Ph)CH_2NMe_2}] with triflic acid, which is leveled to THF-H^+ in tetrahydrofuran solvent, we saw fast disintegration of the complex with elimination of styrene. This decay likely proceeds via the 2-ammoniumalkyl gold intermediate (cf. INT-M2). However, the intermediate is present in too low concentration to be detected by NMR, which suggests that whatever decay route is initiated by protonation, it proceeds fast enough that the intermediate never accumulates enough to produce an observable steady-state concentration. With all the reservations concerning the quantitative accuracy of DFT for these systems, gas-phase DFT calculations identify a transition state for *intramolecular* protodeauration 100.4 kJ/mol (24.0 kcal/mol) above the zero-point energy of the ammonium intermediate (INT-M2), whereas amine elimination required just under 61.5 kJ/mol (14.7 kcal/mol), as depicted in

Figure 5. Considering that *N*-protonation is a pre-equilibrium, the observations suggest that the amine elimination outcompetes the intramolecular protodeauration via the ammonium intermediate.

Mechanism 3: Protonation of the gold(I) center

In addition to protonation of the amine nitrogen or the α-carbon, the protonation of the gold center itself can be considered (*M3* in Scheme 6). Protonation formally oxidizes the d^{10} Au(I) to d^8 Au(III), when the proton (H^+) is counted conventionally as hydride when bound to the metal.[43] This is reminiscent of the first step of a S_N2-type oxidative addition, and hence it could be expected that many metal centers react in this way. Kochi et al. suggested that anionic dialkylaurate(I) complexes undergo protonolysis via hydridogold(III) intermediates, however, they could not observe them.[44] While 2-aminoalkylgold complexes are, in contrast to anionic dialkylaurates, charge-neutral, making their metal centers less electron-rich and less prone to protonation, precedent demands that this mechanism, *M3*, be considered. The formally d^8 Au(III) intermediates have an open coordination site and can be stabilized by accepting a fourth ligand. By DFT the following options were considered: (a) amine nitrogen [cyclic structure] (b) solvent [THF] or (c) counterion [TfO^-]. For (a), we find the hydride intermediate (INT-M3) 95.0 kJ/mol (22.7 kcal/mol) higher in energy than the ammonium intermediate (INT-M2) and another 52.7 kJ/mol (12.6 kcal/mol) are necessary to surmount the activation barrier for protodeauration from INT-M3 by this route (Figure 5). This suggests that even though the hydride intermediate may be formed in principle, the protodeauration does not occur from it. With THF, case (b), the barrier was not lowered enough to render mechanism 3 competitive. For (c) the error of neglecting solvation of the TfO^- anion becomes too large to obtain meaningful energies (see the Supporting Information: Section 6.4).

Hydridoplatinum(IV) intermediates were observed experimentally in protonolysis of square planar d^8 Pt(II) complexes, under certain conditions.[45–47] However, these d^8 Pt(II) species differ from d^{10} Au(I) complexes with regard to the occupied orbitals, i.e. the HOMO, so the analogy may not be relevant. We consider protodeauration via oxidative addition/reductive elimination (S_Eox mechanism, *M3*) to be uncompetitive.

The three mechanisms and their transition states

While literature precedent suggests that there are three distinct mechanisms for a protodeauration of 2-aminoalkyl gold complexes, the computational study, even with our usual caveats with regard to the absolute energies, nevertheless brings an important insight. For two of the three mechanisms, the DFT investigations managed to locate transition state structures, TS-M2 and TS-M3, whose energies above the corresponding intermediates, INT-M2 and INT-M3, indicated significant activation barriers for protodeauration. The same DFT investigation was unable to locate a transition state, TS-M1, for the first mechanism. Figure 6 shows an overlay of the two computed transition states, with the blue structure corresponding to TS-M2 and the yellow to TS-M3. Strikingly, the triangular spatial arrangement of the core atoms, Au, C, and H, is virtually identical for the two transition states, the gross difference being only the Lewis acidic site, Au or H, to which the Lewis basic nitrogen is bound. In fact, if one were to leave the nitrogen unbound altogether, the structure would be the missing TS-M1.

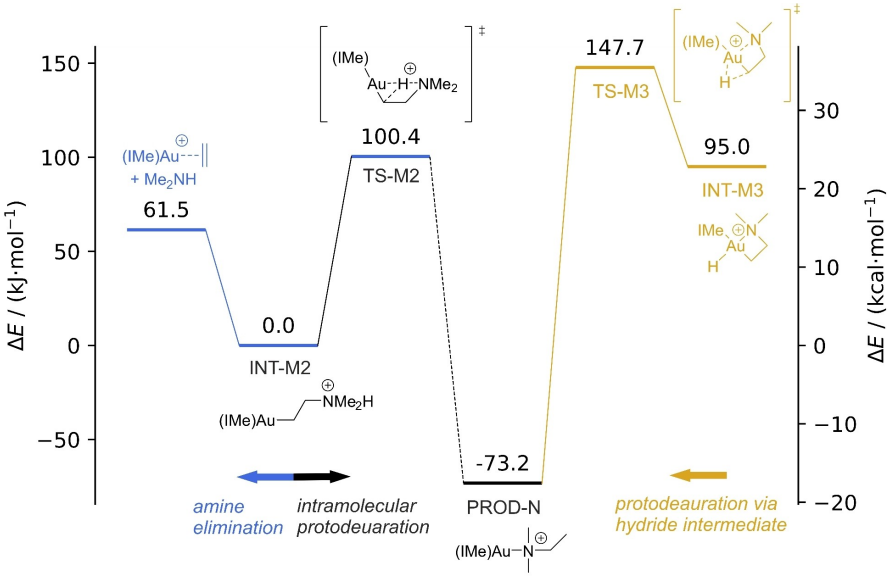

Figure 5. Computed relative energies for intermediates and transition states in protodeauration mechanisms *M2* and *M3*. ZPE-corrected energies relative to the N-protonated intermediate (INT-M2) are computed using PBE0/cc-pVTZ level of theory (see the Supporting Information: Section 6 for details). A van der Waals complex at 58.2 kJ/mol (13.9 kcal/mol) between TS-M2-PROD and PROD-N was omitted and a dashed line was drawn instead.

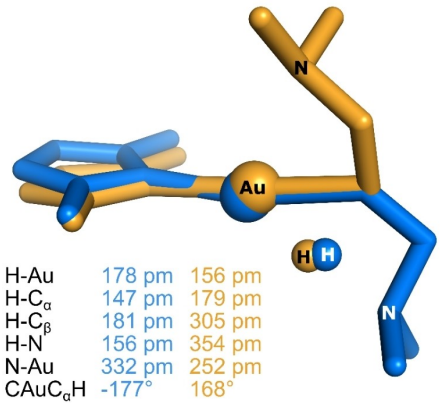

Figure 6. Overlay of the transition state structures for mechanism *M2* (blue) and *M3* (yellow), computed with PBE0/cc-pVTZ.

We presume that the failure to find TS-M1 arises because the open structure collapses to one or the other structures with the Lewis basic nitrogen bound to one or the other Lewis acidic site. Moreover, one can reason that TS-M1 must therefore lie higher in energy than either TS-M2 or TS-M3 because the Lewis acid/Lewis base interaction of the nitrogen with either Lewis acidic site, the Au(I) or the proton, should be exothermic. Accordingly, the computed energies of TS-M2 and TS-M3 set lower bounds for the energy of a hypothetical TS-M1. If neither TS-M2 nor TS-M3 is low enough to make protodeauration competitive with elimination, then a hypothetical TS-M1 is certainly also not low enough, and all of the arguments concerning the site of protonation in a protodeauration step pertain to pre-equilibria prior to a transition state with a triangular Au, C, H arrangement, whichever one it is, TS-M1, TS-M2, or TS-M3, whose energy is just too high.

A further insight becomes evident by inspection of the structures. Both of the computed transition state structures, TS-M2 and TS-M3, show a remarkable resemblance to gem-diaurated structures with a Au–Au bond, if one considers the d^{10} Au(I) cation to be isolobal with a proton. The structural analogy provides a useful qualitative picture. The structurally characterized gem-diaurated complexes with a strong Au–Au bond, featuring an aurophilic interaction, are minima on the potential surface corresponding to isolable species. The interaction of Au(I) with a proton, while significant enough to lead to the same triangular core structure in all three transition states, TS-M1, TS-M2, and TS-M3, is weaker, though, leaving these species as transition states rather than intermediates. The N-protonated intermediate, INT-M2, formed rapidly and reversibly, takes a lower energy route out, namely, elimination of an amine, leaving the Au(I) styrene complex, as we have observed.

Protonation of the π-system in alkenyl gold complexes

Blum and Roth investigated relative protodeauration rates of different organogold compounds.[48] For the protodeauration of a vinyl group they observed a small acceleration by a factor of 4.3 compared to the protodeauration of a methyl group. This acceleration together with a linear Hammett correlation for *para*-substituted aryl gold species was seen indicative for the involvement of the π-system. However, an acceleration of less than an order of magnitude points to a small effect in their system. In line with this, π-electrons were suggested to be involved in the protonolysis of divinylmercury, which is about 100 times as rapid as typical saturated dialkylmercurials.[49] The carbon-carbon double bond in 2-aminoalkenyl groups is conjugated with the nitrogen, and therefore it is more electron-rich than a vinyl group and we expect protonation of the π-system to be correspondingly more favorable. A similar argument can be made when comparing an ordinary olefin to an enamine. Structurally and electronically, protonation of a 2-aminoalkenyl gold complex, the putative intermediate in the hydroamination of an alkyne, leads to a transition state, and a corresponding mechanism, unavailable to the 2-aminoalkyl gold complexes in the previous analysis.

Protonation of the π-system of a 2-aminoalkenyl gold complex produces an α-aurated iminium ion. Such η^1-structures have been observed rather than the η^2-structures for enamine gold complexes.[50] A somewhat similar species has been proposed in the protonation of triphenylvinylmercuric salts, where the two phenyl groups on the β-carbon stabilize the positive charge instead of the nitrogen.[51] For the opposite case of electron-deficient alkenyl groups, computational studies suggested that the π-system be not involved.[52,53] A S_E2 mechanism, similar to *M1*, in which the proton is transported via a water relay was favored for that case instead. A DFT study of a gold-catalyzed hydroamination/cyclization of propargylic alcohols and *o*-phenylenediamine further indicated a difficulty for a direct C–H bond through protodeauration with water without participation of a neighboring iminium π-system.[54]

N-protonation is still possible for 2-aminoalkenyl gold complexes, however, DFT calculations predict larger stability towards elimination compared to 2-aminoalkyl gold complexes. We believe that the combination of slower amine elimination with faster protodeauration via protonation of the π-system makes protodeauration competitive for 2-aminoalkenyl gold complexes. Our analysis suggests the presence of an electron-rich π-system to be a prerequisite for fast protodeauration.

Conclusions

We report the synthesis, isolation, and structural characterization of 2-aminoalkylgold complexes, the putative intermediates in a hypothetical Au-catalyzed hydroamination of alkenes. The reactivity of the complex in solution, and in the gas phase, upon protonation or alkylation, shows loss of a neutral amine, regenerating the olefin complex. Together with our measured alkene and alkyne binding energies to a cationic gold center, the observed decay channel of a 2-ammoniumalkylgold complex – the only product channel observed in solution – indicates that the lower reactivity of alkenes in hydroamination reactions, when compared to alkynes, arises neither because of the differences in the substrate binding affinity nor substrate

activation, but rather because protodeauration cannot compete with amine elimination under the reaction conditions. An analysis of the possible transition states for the non-competitive protodeauration of the 2-ammoniumalkylgold complexes finds structures with 3-center bonding of Au, C, and H which are isolobal to known diaurated structures. In the latter structures, the strong Au–Au interaction, which makes the diaurated structures intermediates, is replaced by the much weaker interaction of the Au center with a proton. Hence the structures with 3-center bonding of Au, C, and H transition states are too high in energy to allow facile protodeauration in competition with amine loss.

Experimental Section

Preparation of [(JohnPhos)Au{CH(Ph)CH_2NMe_2}]: *All the steps of this procedure were performed under exclusion of air and water, either in a glove box or using Schlenk techniques. THF and n-hexane were dried using sodium/benzophenone still. Hamilton syringes and PTFE syringe filters were dried in a vacuum oven at 60 °C.*

A heat gun-dried 50 ml Schlenk-flask was charged with 64 mg KO*t*-Bu (0.57 mmol, 2.0 equiv.) dissolved in 1.6 ml THF. 48 µl *N,N*-dimethyl-2-phenyl-ethanamine (0.28 mmol, 1.0 equiv.) were added using a Hamilton syringe, the solution was cooled down to −78 °C using dry ice/acetone cooling bath and stirred for 0.5 h. 0.35 ml *n*-BuLi (1.6 M solution in hexane, 0.56 mmol, 2.0 equiv.) were added dropwise over 1 min, upon which the color of the solution changed to deep red.

205 mg [(JohnPhos)AuCl] (0.39 mmol, 1.4 equiv.) dissolved in 2.7 ml THF were added dropwise over 5 min under vigorous stirring, accompanied by the change of the solution color to yellow. All dry ice was removed from the cooling bath and the reaction mixture was let warm slowly to −30 °C in the cool acetone. Afterwards, the bath was exchanged for an ice bath and the solvent evaporated *in vacuo*. This resulted in a brownish residue, which was suspended in 7 ml *n*-hexane and the suspension filtered with PTFE Chromafil™ 45 µm syringe filters. The filtrate was then evaporated in the ice bath *in vacuo*. For the purification, the white residue was dried under high vacuum for ca. 5 h, suspended in 2.5 ml n-hexane, filtered with a syringe filter into a vial with a septum and placed into the freezer (-34 °C) in the glove box. After two nights white precipitate formed, which was further triturated two times with 0.5 ml *n*-hexane cooled to −34 °C. The white solid was then dried *in vacuo*, resulting in 161 mg of [(JohnPhos)Au{CH(Ph)CH_2NMe_2}] (64 %). ^{1}H NMR (600.1 MHz, THF-d_8): d(TMS)/ppm = 1.24 (d, 14.2 Hz, 9H, *t*-Bu), 1.34 (d, 14.2 Hz, 9H, *t*-Bu), 2.03 (s, 6H, NMe_2), 2.13–2.19 (m, 1H, CHPh), 2.41 (ddd, 12.1 Hz, 6.0 Hz, 2.2 Hz, 1H, CH_2N), 2.97 (ddd, 12.1 Hz, 11.0 Hz, 4.6 Hz, 1H, CH_2N), 6.55–6.59 (m, 1H), 6.84–6.87 (m, 2H), 6.88–6.91 (m, 2H), 7.06–7.10 (m, 1H), 7.11–7.14 (m, 1H). 7.17–7.20 (m, 1H), 7.28–7.32 (m, 1H), 7.34–7.37 (m, 1H), 7.38–7.40 (m, 1H), 7.43–7.45 (m, 1H), 7.44–7.48 (m, 1H), 7.90–7.94 (m, 1H). ^{13}C NMR (150.9 MHz, THF-d_8): δ(TMS)/ppm = 31.01–31.18 (m, CH_3 of *t*-Bu), 37.44 (d, 17.6 Hz, C_{quart} of *t*-Bu), 37.76 (d, 18.0 Hz, C_{quart} of *t*-Bu), 45.73 (s, NMe_2), 51.79 (d, 80.8 Hz, CHPh), 65.90 (d, 4.1 Hz, CH_2N), 120.72 (d, 1.4,Hz), 127.27 (d, 4.6 Hz), 127.40 (d, ca. 1 Hz), 127.86 (d, 2.5 Hz), 127.92 (s), 128.70 (s), 128.96 (s), 130.24 (s), 130.33 (s), 130.69 (d, 2.1 Hz), 133.51 (d, 7.6 Hz), 136.19 (d, 3.1 Hz), 136.28 (m), 144.17 (d, 5.6 Hz), 151.46 (d, 17.5 Hz), 154.17 (d, 5.6 Hz). ^{31}P NMR (^{1}H-decoupled) (121.5 MHz, THF-d_8): d/ppm = 64.55 (s). HR-ESI-MS m/z = 644.2715 (644.2715 calculated for $C_{30}H_{42}NPAu^+$).

Elemental analysis calcd (%) for $C_{30}H_{41}AuNP$: C 55.99, H 6.42, N 2.18; found: C 55.75, H 6.58, N 2.15. The procedure which employs 1 equiv. *t*-BuLi and 1 equiv. KO*t*-Bu for the deprotonation, as well as detailed characterization, assignments and 2D-spectra, can be found in the accompanying Supporting Information: Section 2.3 and Section 7.3.

NMR titration experiments: In general, a solution of [(JohnPhos)Au{CH(Ph)CH_2NMe_2}] or [(IPr)Au{CH(Ph)CH_2NMe_2}] in a deuterated solvent was treated with a protonating or methylating reagent and NMR spectra were recorded. Details on the NMR titration experiments can be found in the Supporting Information: Section 5.

Mass spectrometry: Typically, solutions of gold complexes were prepared with concentrations of 1–50 µmol/l in membrane-filtered and dry 1,2-dichloroethane. Spray voltages were between 3.5 - 4.5 kV, no sheath or auxiliary gas was used, spray rates were 1–5 µl/min, tube lens voltages set to 50–200 V, capillary temperatures 170–200 °C and 0.5-1.0 mTorr argon was used as collision gas.

General purpose ESI-MS mass spectra, isotope patterns and qualitative CID were measured on a Thermo Finnigan TSQ Quantum triple quadrupole mass spectrometer. Energy-resolved collision-induced dissociation experiments for gold complexes of alkenes and alkynes were performed on a modified Finnigan MAT TSQ-700 tandem mass spectrometer. From the thereby generated data, bond dissociation energies were deconvoluted by the L–CID program.[8] The high resolution ESI-MS were measured by the MS service of the Laboratory for Organic Chemistry of ETH Zurich.

Computational methods: Calculations were performed either using Gaussian 09 (Revision D01),[55] ORCA[56] or xtb quantum chemistry program package.[57] Density functional theory (DFT) level calculations with PBE0[58] or M06 L[59] functionals in conjunction with Dunning's cc-pVDZ or cc-pVTZ basis sets[60,61] were standardly employed. For part of the calculations, semiempirical tight-binding methods as implemented in xtb software, Grimme's D3 correction with Becke-Johnson Damping (BJ),[62,63] resolution of identity approximations (RI)[64] and solvent models were used. Nature of stationary points was confirmed by frequency calculations.

xyz coordinates and further details on the computational workflow are available in the Supporting Information: Section 6.

Supporting Information

MS, NMR; T-CID experimental data (PDF), further comments. Cartesian coordinates of all optimized structures, together with their total and ZPE-corrected energies in Hartree (XYZ).

Acknowledgements

The authors acknowledge financial support from the ETH Zürich and the Swiss National Science Foundation. Open access funding provided by Eidgenössische Technische Hochschule Zürich.

Conflict of Interest

The authors declare no conflict of interest.

Data Availability Statement

The data that support the findings of this study are available in the supplementary material of this article.

Keywords: binding studies · gold catalysis · hydroamination · protodeauration · reaction mechanisms

[1] R. A. Widenhoefer, X. Han, *Eur. J. Org. Chem.* **2006**, *2006*, 4555–4563.
[2] A. S. K. Hashmi, G. J. Hutchings, *Angew. Chem. Int. Ed.* **2006**, *45*, 7896–7936; *Angew. Chem.* **2006**, *118*, 8064–8105.
[3] N. Nishina, Y. Yamamoto, in *Hydrofunctionalization* (Eds.: V. P. Ananikov, M. Tanaka), Springer, Berlin, Heidelberg, **2013**, pp. 115–143.
[4] A. Zhdanko, M. E. Maier, *Angew. Chem. Int. Ed.* **2014**, *53*, 7760–7764; *Angew. Chem.* **2014**, *126*, 7894–7898.
[5] C. Nieto-Oberhuber, M. P. Muñoz, E. Buñuel, C. Nevado, D. J. Cárdenas, A. M. Echavarren, *Angew. Chem. Int. Ed.* **2004**, *43*, 2402–2406; *Angew. Chem.* **2004**, *116*, 2456–2460.
[6] A. L. Reznichenko, K. C. Hultzsch, in *Org. React.* Vol 88 (Ed.: S. E. Denmark), John Wiley & Sons, Inc., **2015**, pp. 1–554.
[7] A. Fürstner, P. W. Davies, *Angew. Chem. Int. Ed.* **2007**, *46*, 3410–3449; *Angew. Chem.* **2007**, *119*, 3478–3519.
[8] S. Narancic, A. Bach, P. Chen, *J. Phys. Chem. A* **2007**, *111*, 7006–7013.
[9] M. Bot, V. Gorbachev, A. Tsybizova, P. Chen, *J. Phys. Chem. A* **2020**, *124*, 8692–8707.
[10] L. Jašíková, J. Roithová, *Organometallics* **2012**, *31*, 1935–1942.
[11] E. Paenurk, P. Chen, *J. Phys. Chem. A* **2021**, *125*, 1927–1940.
[12] C. Unkelbach, H. S. Rosenbaum, C. Strohmann, *Chem. Commun.* **2012**, *48*, 10612–10614.
[13] I. M. Kolthoff, M. K. Chantooni, S. Bhowmik, *J. Am. Chem. Soc.* **1968**, *90*, 23–28.
[14] W. N. Olmstead, Z. Margolin, F. G. Bordwell, *J. Org. Chem.* **1980**, *45*, 3295–3299.
[15] A. Zhdanko, M. Ströbele, M. E. Maier, *Chem. Eur. J.* **2012**, *18*, 14732–14744.
[16] G. Klatt, R. Xu, M. Pernpointner, L. Molinari, T. Quang Hung, F. Rominger, A. S. K. Hashmi, H. Köppel, *Chem. Eur. J.* **2013**, *19*, 3954–3961.
[17] R. D. Bowen, *Acc. Chem. Res.* **1991**, *24*, 364–371.
[18] C. E. Hudson, D. J. McAdoo, *J. Am. Soc. Mass Spectrom.* **2008**, *19*, 1491–1499.
[19] D. J. McAdoo, T. H. Morton, *Acc. Chem. Res.* **1993**, *26*, 295–302.
[20] A. Leyva-Pérez, A. Corma, *Angew. Chem. Int. Ed.* **2012**, *51*, 614–635; *Angew. Chem.* **2012**, *124*, 636–658.
[21] M. Pernpointner, A. S. K. Hashmi, *J. Chem. Theory Comput.* **2009**, *5*, 2717–2725; *J. Chem. Theory Comput.* **2009**, *5*, 2717–2725.
[22] R. Hoffmann, *Angew. Chem. Int. Ed. Engl.* **1982**, *21*, 711–724; *Angew. Chem.* **1982**, *94*, 725–739.
[23] D. Weber, M. A. Tarselli, M. R. Gagné, *Angew. Chem. Int. Ed.* **2009**, *48*, 5733–5736; *Angew. Chem.* **2009**, *121*, 5843–5846.
[24] J. Zhang, C.-G. Yang, C. He, *J. Am. Chem. Soc.* **2006**, *128*, 1798–1799.
[25] C. Brouwer, C. He, *Angew. Chem. Int. Ed.* **2006**, *45*, 1744–1747; *Angew. Chem.* **2006**, *118*, 1776–1779.
[26] T. J. Brown, R. A. Widenhoefer, *J. Organomet. Chem.* **2011**, *696*, 1216–1220.
[27] R. L. LaLonde, W. E. Brenzovich Jr., D. Benitez, E. Tkatchouk, K. Kelley, W. A. Goddard III, F. D. Toste, *Chem. Sci.* **2010**, *1*, 226–233.
[28] A. Fürstner, *Angew. Chem. Int. Ed.* **2018**, *57*, 4215–4233; *Angew. Chem.* **2018**, *130*, 4289–4308.
[29] L. C. Kröger, S. Müller, I. Smirnova, K. Leonhard, *J. Phys. Chem. A* **2020**, *124*, 4171–4181.
[30] J. S. Murray, P. Politzer, *WIREs Comput. Mol. Sci.* **2011**, *1*, 153–163.
[31] W. A. Nugent, J. K. Kochi, *J. Am. Chem. Soc.* **1976**, *98*, 5979–5988.
[32] G. M. Bancroft, T. Chan, R. J. Puddephatt, J. S. Tse, *Inorg. Chem.* **1982**, *21*, 2946–2949.
[33] G. Klopman, *J. Am. Chem. Soc.* **1968**, *90*, 223–234.
[34] M.-E. Moret, D. Serra, A. Bach, P. Chen, *Angew. Chem. Int. Ed.* **2010**, *49*, 2873–2877; *Angew. Chem.* **2010**, *122*, 2935–2939.
[35] J. A. Stone, J. R. M. Camicioli, M. C. Baird, *Inorg. Chem.* **1980**, *19*, 3128–3131.
[36] S. Tshepelevitsh, A. Kütt, M. Lõkov, I. Kaljurand, J. Saame, A. Heering, P. G. Plieger, R. Vianello, I. Leito, *Eur. J. Org. Chem.* **2019**, *2019*, 6735–6748.
[37] W. J. Albery, *Annu. Rev. Phys. Chem.* **1980**, *31*, 227–263.
[38] M. Eigen, *Angew. Chem. Int. Ed. Engl.* **1964**, *3*, 1–19; *Angew. Chem.* **1963**, *75*, 489–508.
[39] J. Hine, in *Adv. Phys. Org. Chem.* Vol. 15 (Eds.: V. Gold, D. Bethel), Academic Press, **1977**, pp. 1–61.
[40] F. O. Rice, E. Teller, *J. Chem. Phys.* **1938**, *6*, 489–496.
[41] H. Matsushita, Y. Tsujino, M. Noguchi, S. Yoshikawa, *Bull. Chem. Soc. Jpn.* **1977**, *50*, 1513–1516.
[42] S. Yoshikawa, H. Matsushita, S. Shibata, in *Biomim. Chem.* (Eds.: D. Dolphin, C. McKenna, Y. Murakami, I. Tabushi), American Chemical Society, **1980**, pp. 49–64.
[43] Compared to most other transition metals, gold is actually more electronegative (2.54) on the Pauling scale for electronegativity than hydrogen (2.20). On the Allen scale, the opposite is true (gold 1.92, hydrogen 2.30). As in a protonation the binding electrons must come from the metal, it is reasonable to speak of an oxidation, irrespective of the problems associated with the definition of a formal oxidation numbers.
[44] A. Tamaki, J. K. Kochi, *J. Chem. Soc. Dalton Trans.* **1973**, 2620–2626.
[45] M. A. Fard, A. Behnia, R. J. Puddephatt, *Organometallics* **2018**, *37*, 3368–3377.
[46] G. S. Hill, L. M. Rendina, R. J. Puddephatt, *Organometallics* **1995**, *14*, 4966–4968.
[47] S. S. Stahl, J. A. Labinger, J. E. Bercaw, *J. Am. Chem. Soc.* **1996**, *118*, 5961–5976.
[48] K. E. Roth, S. A. Blum, *Organometallics* **2010**, *29*, 1712–1716.
[49] M. M. Kreevoy, R. A. Kretchmer, *J. Am. Chem. Soc.* **1964**, *86*, 2435–2440.
[50] M. Sriram, Y. Zhu, A. M. Camp, C. S. Day, A. C. Jones, *Organometallics* **2014**, *33*, 4157–4164.
[51] C. C. Lee, P. J. Smith, *Can. J. Chem.* **1976**, *54*, 3038–3040.
[52] R. BabaAhmadi, P. Ghanbari, N. A. Rajabi, A. S. K. Hashmi, B. F. Yates, A. Ariafard, *Organometallics* **2015**, *34*, 3186–3195.
[53] L. Nunes dos Santos Comprido, J. E. M. N. Klein, G. Knizia, J. Kästner, A. S. K. Hashmi, *Chem. Eur. J.* **2017**, *23*, 10901–10905.
[54] Y. Wang, B. Ling, P. Liu, S. Bi, *Organometallics* **2018**, *37*, 3035–3044.
[55] Gaussian 09, Revision D.01, M. J. Frisch, G. W. Trucks, H. B. Schlegel, G. E. Scuseria, M. A. Robb, J. R. Cheeseman, G. Scalmani, V. Barone, B. Mennucci, G. A. Petersson, H. Nakatsuji, M. Caricato, X. Li, H. P. Hratchian, A. F. Izmaylov, J. Bloino, G. Zheng, J. L. Sonnenberg, M. Hada, M. Ehara, K. Toyota, R. Fukuda, J. Hasegawa, M. Ishida, T. Nakajima, Y. Honda, O. Kitao, H. Nakai, T. Vreven, J. A. Montgomery, Jr., J. E. Peralta, F. Ogliaro, M. Bearpark, J. J. Heyd, E. Brothers, K. N. Kudin, V. N. Staroverov, R. Kobayashi, J. Normand, K. Raghavachari, A. Rendell, J. C. Burant, S. S. Iyengar, J. Tomasi, M. Cossi, N. Rega, J. M. Millam, M. Klene, J. E. Knox, J. B. Cross, V. Bakken, C. Adamo, J. Jaramillo, R. Gomperts, R. E. Stratmann, O. Yazyev, A. J. Austin, R. Cammi, C. Pomelli, J. W. Ochterski, R. L. Martin, K. Morokuma, V. G. Zakrzewski, G. A. Voth, P. Salvador, J. J. Dannenberg, S. Dapprich, A. D. Daniels, Ö. Farkas, J. B. Foresman, J. V. Ortiz, J. Cioslowski, and D. J. Fox, Gaussian, Inc., Wallingford CT, **2009**.
[56] F. Neese, *WIREs Comput. Mol. Sci.* **2018**, *8*, e1327.
[57] C. Bannwarth, E. Caldeweyher, S. Ehlert, A. Hansen, P. Pracht, J. Seibert, S. Spicher, S. Grimme, *WIREs Comput. Mol. Sci.* **2021**, *11*, e1493.
[58] C. Adamo, V. Barone, *J. Chem. Phys.* **1999**, *110*, 6158–6170.
[59] Y. Zhao, D. G. Truhlar, *J. Chem. Phys.* **2006**, *125*, 194101.
[60] T. H. Dunning, *J. Chem. Phys.* **1989**, *90*, 1007–1023.
[61] R. A. Kendall, T. H. Dunning, R. J. Harrison, *J. Chem. Phys.* **1992**, *96*, 6796–6806.
[62] S. Grimme, *WIREs Comput. Mol. Sci.* **2011**, *1*, 211–228.
[63] S. Grimme, S. Ehrlich, L. Goerigk, *J. Comput. Chem.* **2011**, *32*, 1456–1465.
[64] F. Weigend, *Phys. Chem. Chem. Phys.* **2006**, *8*, 1057–1065.

Manuscript received: February 2, 2022
Accepted manuscript online: March 23, 2022
Version of record online: May 27, 2022